ENGLISH VERSION

Characterization of blast furnace slag for road projects

Caracterización de una escoria de alto horno para proyectos viales

H. Rondón [1]*, W. Fernández *, D. Patiño *, J. Ruge **, H. Vacca ***, F. Reyes ***

* Universidad Distrital Francisco José de Caldas, Bogotá. COLOMBIA
** Universidad Piloto de Colombia, Bogotá. COLOMBIA
*** Pontificia Universidad Javeriana, Bogotá. COLOMBIA

Fecha de Recepción: 07/09/2017
Fecha de Aceptación: 09/03/2018
PAG 83-92

Abstract

The present study evaluated the potential use of Blast Furnace Slag (BFS) as forming material of untreated granular layers in pavement (e.g. base, subbase and subgrade), and as stone aggregate in the manufacture of asphalt mixtures. For that purpose, tests of characterization, X-ray diffractometry (XRD), X-ray fluorescence (XRF) and imaging in a scanning electron microscope (SEM) were executed on the BFS. As a general conclusion is reported that the BFS can be used in the formation of unbound granular layers of subbase. As granular base material, its use would be recommended on roads with low traffic volumes or with thick asphalt layers and as a selected material, in tertiary roads that support light traffic. In the case of HMA is not recommended to use the coarse fraction of the BFS as a stone aggregate. However, the obtained results indicate that the fine fraction shows good characteristics to be used in the production of the mastic of such mixtures.

Keywords: *Blast furnace slag, BFS, granular material, road construction, pavements*

Resumen

El presente estudio evaluó el potencial de uso de una escoria de alto horno (BFS) como material de conformación de capas granulares no tratadas en pavimentos (base, subbase y afirmado), y como agregado pétreo en la fabricación de mezclas asfálticas. Para tal fin, fueron ejecutados sobre la BFS, ensayos de caracterización, difractometría de rayos X (DRX), fluorescencia de rayos X (FRX) e imagenología en un microscopio electrónico de barrido (MEB). Como conclusión general se reporta que la BFS puede ser utilizada en la conformación de capas granulares no tratadas de subbase. Como material para base granular se recomendaría su uso en vías con bajos volúmenes de tráfico o con capas asfálticas gruesas, y como material de afirmado, en vías terciarias que soporten tráfico liviano. Para el caso de mezclas asfálticas no se recomienda utilizar como agregado pétreo la fracción gruesa de la BFS. Sin embargo, los resultados obtenidos indican que la fracción fina presenta buenas características para ser utilizado en la producción del mastic de dichas mezclas.

Palabras clave: Escoria de alto horno, BFS, material granular, construcción vial, pavimentos

1. Introduction

In construction, maintenance and road rehabilitation projects, large quantities of natural granular materials (NGM) are used. This results in a negative environmental impact. In the last two decades, the interest in replacing NGM with alternative materials has been growing in order to conserve natural resources, reduce the space they occupy in the dumps at the end of their useful life and prevent the deterioration of the landscape (Pasetto and Baldo, 2010). However, with regard to the use of alternative materials, various concerns related to the assessment of technical and environmental performance in road projects still exist. These concerns have not been answered in a satisfactory manner (Nouvion et al., 2009).

One of the alternative materials that can be used as NGM substitutes is the Blast Furnace Slag (BFS). This material is formed when iron ore, coke and a flux (either limestone or dolomite) are fused together in a blast furnace (FHWA, 2008; Marriaga and Claisse, 2011). Significant quantities of this material are generated as waste on a daily basis in iron industries. According to Okumura (1993), Proctor et al. (2000) and Airey et al. (2004), the annual production of BSF in the USA, Japan and the UK is 13, 24.3 and 4 million tons respectively. According to Proctor et al. (2000), and Das et al. (2007), for every ton of produced steel, a quantity between 220-370 kg and 340-421 kg of blast furnace slag is produced respectively. The conventional method of eliminating slag is to transport it and deposit it in dumps. This causes an environmental problem since is occupies spaces in the landfills, thus wasting a material that can be reused. According to Nouvion et al. (2009), using blast furnace slag could reduce the energy consumption during the process of NGM extraction, thus reducing the release of pollutants into the air, water and soil.

Some uses of the BFS include fertilizers (Geiseler, 1996), road construction (Houben et al., 2010), soil recovery and preparation of materials such as glass-ceramics, silica gel, bricks, etc. (Das et al., 2007). However, perhaps its broader use is the production of cement (Shi, 2004; Das et al., 2007; Abu-Eishah et al., 2012; Sorlini et al., 2012).

The study group identified as possible uses of BFS for the substitution of MGN in road projects, the formation of granular layers of subgrade, subbase and base, and as stone aggregates for the manufacture of asphalt mixtures. Therefore, in the present study, an experimental phase was performed in order to assess these possible uses. For this purpose, the typical tests conducted on the coarse and fine fractions of NGM for

[1] *Corresponding author:*

Facultad del Medio Ambiente y Recursos Naturales, Universidad Distrital Francisco José de Caldas, Bogotá, Colombia.
E-mail: harondonq@udistrital.edu.co

their characterization were carried out on the BFS. In contrast to other studies carried out on the BFS, in the present study the mineralogical, chemical and microstructural composition was measured through X-ray diffractometry (XRD), X-ray fluorescence (XRF) and visual recognition techniques in a scanning electron microscope (SEM).

2. Methodology

The BFS used was the type of Air-Cooled Blast Furnace Slag - ACBFS (once the slag is out of the blast furnace, it is slowly cooled in the open air; NSA, 2016), from the company Acerías Paz del Río (Nobsa – Boyacá, Colombia). Figure 1 shows the coarse and fine fractions of the analyzed BFS.

Figure 1. *Slag particles (coarse and fine)*

2.1 Visual characterization

A phase of visual characterization was initially made to help to identify the groups of representative samples that would be tested in XRD, XRF and SEM. This is because the BFS is a highly heterogeneous material (shapes and sizes of particles, chemical constitution, texture, specific gravity, degradation resistance and porosity, etc.) that develops complex characteristics and properties (Akbarnejad et al., 2014). The two types of coarse particles that predominate in the BFS used in the present study are shown in figure 2. The particles of the image on the left are those present in larger quantities within the BFS (on average, approximately 65% with regard to the number of particles), their surface color is shiny black, and when they are ground they internally develop a grayish color. In addition, they have a rigid and hard consistency and a mass similar to the natural stone aggregates (NGM), even though they are much more porous. On the contrary, the particles of the image on the right are easy to degrade through abrasion (even with the hands); they are lightweight, light green and can float in water.

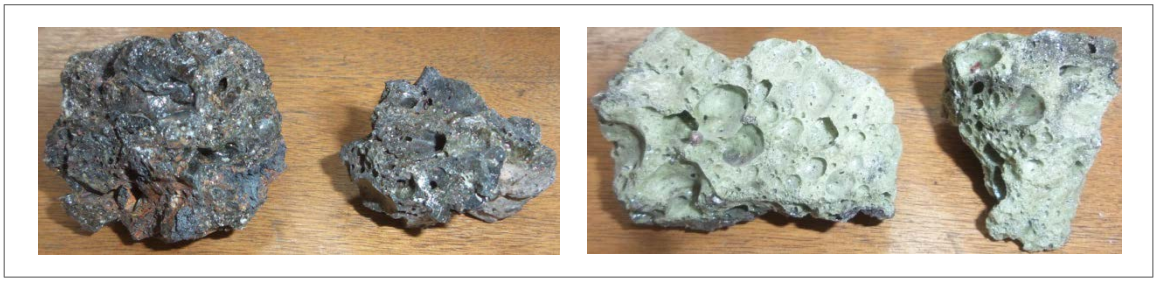

Figure 2. *Slag particles (size between ¾" and 1" in diameter)*

2.2 Typical characterization by specifications

The same tests specified to the NGM were carried out on the BFS in the construction of untreated granular layers in pavements (base, subbase, subgrade, etc.) and the manufacture of asphalt mixtures such as: specific gravity and absorption (AASHTO T 84-00, AASHTO T 85-91), degradation of Los Angeles machine (AASHTO T 96 – 02), Micro-Deval (AASHTO T327-05), 10% of fines (DNER-ME 096-98), impurity content (UNE 14613:2000), plasticity index (ASTM D 4318-00), flat and elongated indices (NLT 354-91), sand equivalent (AASHTO T 176-02) and CBR (AASHTO T 193-99). Every test was conducted five times and no high dispersion was generated in the results. To conduct the CBR test, the grading presented in Table 1 were used (BG, SBG and A refer to the base, subbase and subgrade, respectively). Prior to this test, the samples were compacted through the Proctor test (AASHTO T 180), obtaining maximum dry unit weights and optimum water contents of 16 kN/m3 and 6%, 16.6 kN/m3 and 7.1%, and 16.2 kN/m3 and 7.7% for BG, SBG and A, respectively.

Table 1. *Granulometry used for compaction tests and CBR (INVIAS, 2013)*

Sieve		Percentage that passes (%)		
		BG-25	**SBG-38**	**A-38**
1 ½″	37.5 mm	-	100	100
1″	25 mm	100	85	-
¾″	19 mm	85	70	90
3/8″	9.5 mm	65	60	72.5
No. 4	4.75 mm	50	45	52.5
No. 40	2.0 mm	32.5	32.5	40
No. 80	0.425 mm	20	19	21.5
No. 200	0.075 mm	10	8.5	13.5

2.3 Mineralogical characterization

For the mineralogical characterization of the BFS, an analysis based on X-ray diffractometry (XRD) and X-ray fluorescence (XRF) was carried out. In the XRD test, the preparation of the sample began with a pulverizing and sieving phase in order to guarantee a particle size smaller than 75µm. After that, the sample was poured on an aluminum sample holder and with the help of a spatula the excess was removed, thus creating a flat surface on which the analysis was carried out (please refer to the details of the procedure in Moore and Reynolds, 1997; Chipera and Bish, 2001; Zhang et al., 2003 and Reed, 2005).

In the case of the XRF test (Beckhoff et al., 2006), the samples were dried at 105°C for a 12-hour period. Since the grain size of the sample was too coarse and its grading was well graded (heterogeneous), this was reduced in an agate ball mill. The samples were homogenized by agitation and were prepared in the shape of meltedpearls with a sample: flux ratio of 1:10. A mixture of lithium tetraborate and lithium metaborate was used as a flux and lithium iodide was added in order to prevent the samples from sticking. After that, the samples were taken to an induction furnace. In doing so, glass disks of 37 mm in diameter were obtained to be measured in a semi-quantitative or quantitative application. The quantitative analysis was carried out through the SemiQ software, with which 11 scannings were performed in order to detect all the elements present in the sample (H, C, Li, Be, B, N, O are excluded as well as the transuranic elements).

2.4 Microstructure

The microstructure of any material that is a component of a system that will work mechanically, governs part of its operation, especially if this microstructure is susceptible to be invaded by a fluid that conditions its mechanic and hydraulic response. The preparation of the slag samples for an imaging test was conducted through the first selection of different grains in order to obtain a statistically reliable result. The chosen grains were five green grains, three black grains and one white grain. This last grain was scarce in the delivered population; therefore, a single sample was selected. The assembly of the sample consisted in the use of resin and hardener to obtain a sample containing all the grains chosen. After that, the surface of interest was mirror polished (abrasives in disks and cloths) and then a conductive layer was deposited on the surface. The final result of the previous metallization is shown in Figure 3. Finally, the sample was studied by using a scanning electron microscope (SEM) and several photographs were taken of every individual grain at different zooms to be subsequently analyzed. In order to compare the results obtained on the BFS, this test was also conducted on an NGM sample used as a stone aggregate of asphalt mixtures and that has been extensively studied and characterized by the research group (Figure 4).

Figure 3. *Sample assembled with selected grains of BFS*

Figure 4. *Sample assembled with selected grains of NGM*

3. Results

3.1 Typical characterization by specifications

The results of the characterization tests conducted on the BFS are detailed in Table 2.

It is shown in Table 2 that by decreasing the size of the BFS particles, the specific gravity increases and the absorption decreases. This is perhaps due to the fact that during the process of mechanical fracturing performed on the coarse particles to obtain fine particles the latter lose part of their porosity. In addition, the above is an indicator of an increase in porosity with the increase in the size of the particle. Based on the degradation results in Micro-Deval and 10% of fines, the BFS is reported to present a good resistance to abrasion degradation by friction between particles and to the fracturing under monotonic loading, respectively. However, as reported in the reference literature (e.g., Airey et al., 2004; FHWA, 2008), the BFS is a material that experiences low resistance to abrasion degradation by impact in Los Angeles machine. In addition, it can be observed that this material presents particles with ideal shapes (rounded with angular and cracked sides with very little content of elongated and flat particles) to develop a good granular skeleton that helps in the compaction processes, as well as resisting static, dynamic or impact loading. The fine particles do not present any content of clay, organic matter or dust. The CBRs obtained (at 100% of maximum dry density and four-day immersion in water) were 95.3%, 88.7% and 76.1% for BG, SBG and A, respectively. These dimensions are high and, together with the results previously reported in Table 2 and the minimum quality requirements required for BG, SBG and A (Table 3) indicate that the BFS can be used as stone aggregate for the formation of granular layers of subbase, subgrade of pavements. We could even think of its use as material for the granular base of roads with low traffic volumes or with thick asphalt layers, since only it does not comply with the required maximum resistance of 35% of degradation in Los Angeles machine. Additionally, in the case of subgrade, caution is required since this material would be susceptible to fracture (according to the obtained values of degradation in Los Angeles machine and the high porosity of coarse particles) because these layers are subjected to the direct action of traffic in tertiary roads.

Table 2. *BFS characterization*

Test	*Method*	*Value*
Specific gravity/absorption (¾")	*AASHTO T 84-00* *AASHTO T 85-91*	*1.81/3.75%*
Specific gravity/absorption (3/8")		*1.97/3.33%*
Specific gravity/absorption (No. 4)		*2.11/2.73%*
Specific gravity/absorption (No. 40)		*2.26/2.65%*
Specific gravity/absorption (No. 80)		*2.36/2.25%*
Specific gravity/absorption (No. 200)		*2.45/1.95%*
Resistance of Los Angeles machine, 500 revolutions	*AASHTO T 96 – 02*	*49.2%*
Micro-Deval	*AASHTO T327-05*	*29.2%*
10% of fines (dry)	*DNER-ME 096-98*	*123 kN*
Cracked sides: 1 side	*ASTM D 5821-01*	*92%*
Cracked sides: 2 sides		*88%*
Flat and elongated particles		*1%*
Sand equivalent	*AASHTO T 176-02*	*62%*
Impurity content	*UNE 14613 : 2000*	*0%*
Plasticity index	*ASTM D 4318-00*	*Non plastic*
Flattening index	*NLT 354-91*	*5.62%*
Elongated index		*10.62%*

As coarse stone aggregate in the case of asphalt concrete mixtures (DHM – dense hot mix) the high adsorption reported in Table 2 shows the need to require higher contents of asphalt, thus resulting in an increase in cost. Despite the above, in some cases, this higher cost could be compensated with higher performance (volume per mass) of BFS as an aggregate due to the lower unit weight of the mixture. Since this is a porous material in comparison with conventional aggregates, it could be necessary a longer drying period in asphalt mixture production plants. In addition, since the BFS does not comply with most of the minimum quality requirements for DHM (Table 3), the BFS will be more prone to abrasion degradation and particle fracturing since the vehicles are driven directly on the asphalt layer in the pavement. However, the BFS is observed to have desirable properties for being used as an aggregate that can substitute the fine fraction of the stone aggregate (high sand equivalent, non-plastic filler, zero impurity content and adsorption decrease).

Table 3. *Minimum quality requirements of stone aggregates for subgrade (A), subbases (SBG), bases (BG) and asphalt mixtures (DHM) according to INVIAS (2013). High-traffic volume roads*

Test	Method	A	SBG	BG	MDC
Degradation Los Angeles (500 revolutions), dry	AASHTO T 96-02	50% máx.	50% máx.	35% máx.	25% max.
Micro-Deval	AASHTO T327-05	NA	30% máx.	30% máx.	20% max.
10% of fines (dry)	DNER-ME 096-98	NA	NA	90 kN mín.	110 kN min.
Plasticity index	ASTM D 4318-00	4-9	6% máx.	0	0
Sand equivalent	AASHTO T 176-02	NA	25% mín.	30% mín.	50% min.
Impurity content	UNE 14613 : 2000	2% máx.	2% máx.	2% máx.	0.5% max.
Cracked sides: 1 side	ASTM D 5821-01	NA	NA	100% mín.	85% min.
Cracked sides: 2 sides	ASTM D 5821-01	NA	NA	70% mín.	70% min.
Flattening index	NLT 354-91	NA	NA	35% máx.	10% max.
Elongated index	NLT 354-91	NA	NA	35% máx.	10% max.
CBR (at 100% of maximum dry density and four-day immersion in water)	INV. E-148	15% mín.	30% mín.	95% mín.	NA

Note: NA: Not applicable

3.2 Mineralogical Characterization – XRD and XRF

In Figure 5, the diffractogram (powder sample) obtained from the XRD is shown. The counts ordinate axis can be observed. This corresponds to the intensities of each diffracted mineral peak and the abscissas show the 2theta angle according to the Bragg law (Equation 1).

$$n\lambda = 2d \operatorname{sen} \vartheta \qquad (1)$$

Where, n is a positive integer, λ is the wavelength of the incident wave, d is the interplanar spacing, and ϑ is the diffraction angle. Bragg (1910) showed that there is a ratio between the interplanar spacing d in the crystal structure of a mineral or minerals and the sine of the ϑ angle. The intensity of the peak height in the y axis depends on the crystal structure and the quantity of each mineral present in the sample

In other words, the different peaks detected are the plane reflections in each mineral phase, which are compared with a data basis (Brucker). The quantification is carried out with specialized software, which operates under the RIR method. This particular method consists of making a ratio between relative intensities. The function modeling the diffractogram takes into account the scale parameters, which described the background and the shapes of the peaks, instrument contributions and preferred orientations. In Table 4 it is possible to observe the minerals found in the analyzed BFS sample.

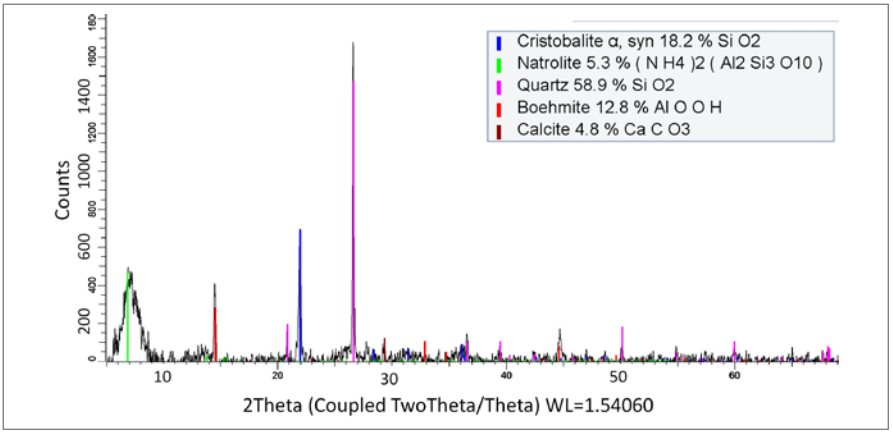

Figure 5. *Powder BFS diffractogram*

Table 4. *Mineral percentages in the sample*

Mineral	***Weight%***
Quartz	*58.9*
Cristobalite	*18.1*
Boehmite	*12.8*
Calcite	*4.8*
Natrolite	*5.3*

It can be observed that the predominant minerals (77%) are quartz (silica - SiO_2) and cristobalite (high-temperature cubic phase of silica - SiO_2). The silica is one of the most abundant oxide materials in nature, where it can exist in an amorphous manner as glass silica or in a wide variety of crystal shapes. This material has good resistance to abrasion (high hardness), high thermal stability and generally acceptable mechanical properties (Table 5), as reported by Muniandy et al. (2013). The presence of silica in all its shapes in BFS samples can possibly generate high interlocking levels, either between its own particles or working in combination with NGM due to its rough texture and compression. The results in XRD are consistent with those reported in the XRF test (Table 6), where the predominant chemical component is silica (SiO_2) in the shape of Quartz and Cristobalite. In addition, the analyzed BFS is reported to be comprised mainly of silica, calcium oxide (CaO) and aluminum oxide (86.76%).

In the case of asphalt mixtures, the Al_2O_3 together with CaO can be used as adhesion improves (Muniandy et al., 2013; Modarres and Rahmanzadeh, 2014; Nassar et al., 2016). Additionally, the SiO_2 and Al_2O_3 are pozzolanic compounds, which in sizes of very fine particles can develop self-cementing properties (Misra et al., 2005). All of the above could result in beneficial effects on the resistance to rutting, moisture damage and stripping.

Table 5. *Physical properties of quartz*

Property	***Quartz***
Density (g/cm3)	*2.65*
Tensile Strength (MPa)	*55*
Compressive Strength (MPa)	*2070*
Elasticity Modulus (GPa)	*70*

Table 6. *XRF results for the sample analyzed in dry base*

Element	***SiO_2***	***CaO***	***Al_2O_3***	***Fe_2O_3***	***MnO***	***TiO_2***	***K_2O***	***MgO***	***Na_2O***	***SO_3***	***Ba***	***Cr***
Weight % of the Sample	*52.03*	*20.83*	*13.90*	*6.52*	*2.26*	*0.979*	*0.862*	*0.818*	*0.653*	*0.475*	*0.209*	*0.124*

3.3 Microstructure

The difference between the three colors chosen from the beginning in the BFS effectively showed three different populations. Initially, the porosity of the samples was calculated in order to obtain the results shown in Table 7. The green grains have a significant dispersion, but they tend to present dimensions above other populations with regard to porosity. In white grains, the porosity is high, but it is less than in the case of the green population. Finally, the black population stands out for its reduced porosity and minor variation.

Table 7. *Porosity values calculated for different grain populations*

Type	*Porosity (%)*	*Error (%)*
Green Grains	*63*	*13*
Black Grains	*9*	*3*
White Grain	*50*	*4*

In order to visually understand the results, it was necessary to conduct SEM tests. Figures 6, 7 and 8 show specific and representative cases of each grain sample chosen. It is possible to demonstrate the difference between the black grain samples and the other types of grains. In the images shown it can be analyzed that the most frequent grain populations in the sample (green and white) have a similar porosity (63% and 50%), revealed by the presence of coarser grains. In contrast, the black grain has a lower porosity as shown in Figure 7. The quantitative values of the pore throats of each population are consistent with the porosity obtained since the lower the percentage of voids content in the sample, the fewer opportunities of interconnection among them. In addition, in the case of black grains, it can be demonstrated that the low porosity present in the sample is translated into a lower value in the proportion and size of the throats (Table 8). The distribution of the pore throats of the black grain population is not well defined due to the low porosity observed in the image, largely controlled by the size of the grain that tends to be smaller than in the other populations. On the other hand, both green and white grains show a distribution that can be visually defined with ease in the images since the connectivity between the pores is clearly shown. Table 8 shows the statistical summary for each population. Again, the variation in the results of green grains is evident by means of a significant deviation. However, it reveals a higher average in the pore throat in comparison with the other grains. Statistically, it can be determined that for green, black and white grains, the pore throat average is 82.6 µm, 27.5 µm and 30.3 µm, respectively.

Based exclusively on the imaging and the pore throat analysis, it is evident that the population of green grains governs the behavior of the whole sample since its grains present matches near 72% of the total population. This result is contrary to that obtained in the visual characterization of coarse particles, where a greater quantity of black and grayish grains was reported. This is perhaps because, during the process of mechanical fracturing to obtain fine particles, the coarse green particles of the BFS are easier to degrade and fracture. The green grains of the BFS present high porosity, which makes us assume a priori that if this material is part of an asphalt mixture, the binding material will adhere more easily to them.

Seven types of grain were selected to conduct the test on the NGM, which represented different lithological characteristics, they did not have shared characteristics, and they were classified according to the size, color and sphericity of the grain. The average porosity and pore throat of the selected grains were 7% and 12 µm, respectively. These average porosity and pore throat dimensions are low in comparison with those previously reported in the BFS.

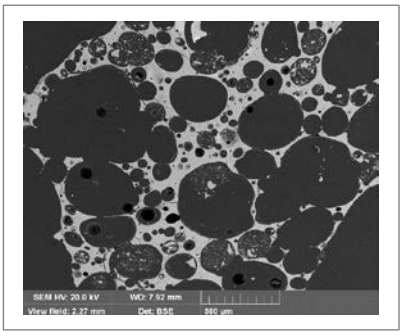

Figure 6. *Representative grain of the green grain population*

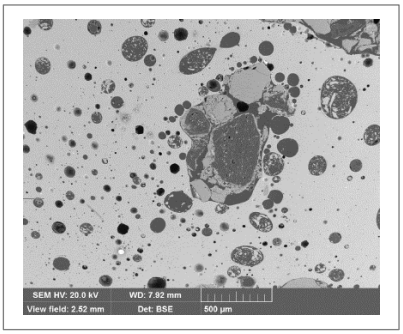

Figure 7. *Representative grain of the black grain population*

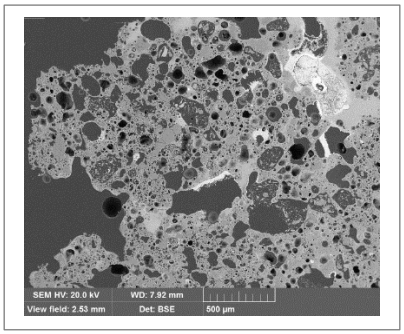

Figure 8. *Representative grain of the white grain population*

Table 8. *Statistical data for each grain population*

Parameter	*Green Grains*	*Black Grains*	*White Grains*
Average (µm)	*82.6*	*27.5*	*30.3*
Deviation (µm)	*71.0*	*25.0*	*25.4*
Median (µm)	*60*	*17.65*	*20.5*
Range (µm)	*575.9*	*99.3*	*112.7*
Maximum (µm)	*585.9*	*104.0*	*116.6*
Minimum (µm)	*10.0*	*4.7*	*3.9*
Counts	*255*	*39*	*60*

4. Conclusions

Based on the results obtained in the case of the use of BFS as a material in the formation of granular layers, we can conclude the following:

Since the analyzed BFS is mainly comprised of Quartz (silica), which is a high hardness material, it shows good resistance to abrasion degradation by friction and fracturing under monotonic loading. In addition, it has other characteristics that are desirable in road projects, such as i) particles predominantly rounded with angular and cracked sides and very little content of elongated and flat particles (indicators of a more compact granular skeleton which is less deformable under mechanical loading). ii) high sand equivalent (an indicator of a material that will not have an excess of fines), iii) the fine particles do not present any content of clay or organic material (these two materials tend to decrease the mechanical response of granular materials in road projects), iv) high shear resistance under controlled humidity and density conditions. However, the high porosity of the particles can lead to fracturing under a mechanical loading. As a result of the aforementioned properties, the BFS can be used with confidence in the formation of subbase granular layers in pavements (since the traffic efforts have dissipated when they act on this layer), as granular base material of roads with low traffic volumes or with thick asphalt layers, and as a subgrade in tertiary roads supporting light traffic (it is not recommended

for heavy traffic since this layer in tertiary roads generally support traffic directly).

In the case of asphalt mixtures, we can come to the conclusion that the coarse fraction of the BFS cannot be used since this does not meet the minimum quality requirements for the manufacture of these materials according to technical specifications. In addition, the coarse particles present high porosity and thus high adsorption. The latter is an indicator of i) probability of particle fracturing by impact or under the action of heavy traffic and cyclic loading, ii) need of higher contents of asphalt, resulting in cost increase, iii) higher requirements of drying times of BFS particles in the mixture production plants. Despite the above, the fine fraction reports good characteristics to be used in the production of asphalt mix mastic: i) high sand equivalent, ii) zero content of clay or organic material, iii) since the fine fraction is mainly comprised of pozzolanic materials, CaO y Al_2O_3 it can develop self-cementing properties thus increasing the resistance to moisture damage and stripping, improving the superficial asphalt-subgrade adhesion, the inner unity of the mastic, and the resistance of the mixture to rutting, iv) the high content of quartz identified reveals that a high mechanical resistance and interlocking can be developed in the skeleton of the collection of materials.

5. References

***Abu-Eishah S. I., El-Dieb A. S., Bedir M. S. (2012)**, Performance of concrete mixtures made with electric arc furnace (EAF) steel slag aggregate produced in the Arabian Gulf region. Construction and Building Materials, 34:249-256, http://dx.doi.org/10.1016/j.conbuildmat.2012.02.012.*

***Airey G. D., Collop A. C., Thom N. H. (2004)**, (12-16 of September). Mechanical performance of asphalt mixtures incorporating slag and glass secondary aggregates. In Proceedings of the 8th Conference on Asphalt Pavements for Southern Africa (CAPSA'04). Sun City, North West Province, South Africa.*

***Akbarnejad S., Houben L.J.M., Molenaar A.A.A. (2014)**, Application of aging methods to evaluate the long-term performance of road bases containing blast furnace slag materials. Road Materials and Pavement Design, 15(3):488-506, http://dx.doi.org/10.1080/14680629.2014.907196.*

***Beckhoff, B., Kanngießer B., Langhoff N., Wedell R., Wolff H. (2006)**, Handbook of Practical X-Ray Fluorescence Analysis, 863 p., Springer.*

***Chipera S., Bish D. (2001)**. Baseline studies of the clay minerals society source clays: powder x-ray diffraction analysis. Clays and Clay Minerals, 49(5):398-409, DOI: 10.1346/CCMN.2001.0490507.*

***Das B., Prakash S., Reddy P. S. R., Misra V. N. (2007)**, An overview of utilization of slag and sludge from steel industries. Resources, Conservation and Recycling, 50(1):40-57. http://dx.doi.org/10.1016/j.resconrec.2006.05.008.*

***FHWA (2008),** Federal Highway Administration Research and Technology. Coordinating, Developing, and Delivering Highway Transportation Innovations. User Guidelines for Waste and Byproduct Materials in Pavement Construction. Report Publication Number: FHWA-RD-97-148.*

***Geiseler J. (1996),**. Use of steelworks slag in Europe. Waste Management, 16(1-3):59-63. doi:10.1016/S0956-053X(96)00070-0.*

***Houben L. J. M., Akbarnejad S., Molenaar A. A. A. (2010)**, (3-5 of June). Performance of pavements with blast furnace base courses. In GeoShanghai 2010 - International Conference, Paving Materials and Pavement Analysis, Geotechnical Special Publication No. 203 (pp. 476-483). Shanghai, China.*

***INVIAS (2013)**, Instituto Nacional de Vías –Especificaciones Generales de Construcción de Carreteras. Bogotá D.C., Colombia.*

***Marriaga J. L., Claisse P. (2011)**, The influence of the blast furnace slag replacement on chloride penetration in concrete. Ingeniería e Investigación, 31(2):38-47.*

***Misra A., Biswas D., Upadhyaya S. (2005)**, Physico-mechanical behavior of selfcementing class C fly ash–clay mixtures. Fuel, 84(11):1410–1422, http://dx.doi.org/10.1016/j.fuel.2004.10.018.*

***Modarres A., Rahmanzadeh M. (2014)**, Application of coal waste powder as filler in hot mix asphalt. Construction and Building Materials, 66:476–483, http://dx.doi.org/10.1016/j.conbuildmat.2014.06.002.*

***Moore D., Reynolds R. (1997),** X-Ray diffraction and the identification and analysis of clay minerals, p. 378, New York: Oxford University Press, Second Edition.*

***Muniandy R., Aburkaba E., Mahdi L. (2013),** Effect of mineral filler type and particle size on asphalt-filler mastic and stone mastic asphalt laboratory measured properties. Australian Journal of Basic and Applied Sciences, 7(11):475-787.*

***Nassar A. I., Mohammedb M. K., Thom N., Parry T. (2016)**, Mechanical, durability and microstructure properties of Cold Asphalt Emulsion Mixtures with different types of filler. Construction and Building Materials, 114:352–363, http://dx.doi.org/10.1016/j.conbuildmat.2016.03.112.*

***Nouvion S., Jullien A., Sommier M., Basuyau V. (2009)**, Environmental modeling of blast furnace slag aggregate production. Road Materials and Pavement Design, 10(4):715-745, http://dx.doi.org/10.1080/14680629.2009.9690224*

***NSA (2016)**, National Slag Association. http://nationalslag.org/blast-furnace-slag, consulted in april of 2016.*

***Okumura H. (1993)**, Recycling of iron-and steelmaking slags in Japan. In: Proceedings of the 1st International Conference on Processing Materials for Properties, Sponsored by: TMS; MMIJ Publ by Minerals, Metals & Materials Soc (TMS) (pp. 803-806).*

***Pasetto M., Baldo N. (2010)**, Experimental evaluation of high performance base course and road base asphalt concrete with electric arc furnace steel slags. Journal of Hazardous Materials, 181(1-3):938–948, http://dx.doi.org/10.1016/j.jhazmat.2010.05.104.*

***Proctor D. M., Fehling K. A., Shay E. C., Wittenborn J. L., Avent C., Bigham R. D., Connolly M., Lee B., Shepker T. O., Zak M. A. (2000)**, Physical and chemical characteristics of blast furnace, basic oxygen furnace, and electric arc furnace steel industry slags. Environmental Science and Technology, 34(8):1576-1582, DOI: 10.1021/es9906002.*

***Reed S. J. B. (2005)**, Electron Microprobe analysis and Scanning Electron Microscopy in Geology, 190 p., New York: Cambridge University Press.*

***Shi C. (2004)**, Steel slag—its production, processing, characteristics, and cementitious properties. Journal of Materials in Civil Engineering, 16(3):230-236, http://dx.doi.org/10.1061/(ASCE)0899-1561(2004)16:3(230).*

***Sorlini S., Sanzeni A., Rondi L. (2012)**, Reuse of steel slag in bituminous paving mixtures. Journal of Hazardous Materials, 209–210:84-91, http://dx.doi.org/10.1016/j.jhazmat.2011.12.066.*

***Zhang G., Germaine J., Torrence M., Whittle A. (2003)**, A simple sample-mounting method for random powder X-RAY diffraction. Clays and Clay Mineral, 51(2):218-255, DOI: 10.1346/CCMN.2003.0510212.*